THERMODYNAMIC EVALUATION OF AN ORC TEST RIG - FROM COMPREHENSIVE EXPERIMENTAL RESULTS TO A SIMULATION MODEL

Tobias Popp[1]*, Florian Heberle[1], Andreas P. Weiß[2] and Dieter Brüggemann[1]

[1] University of Bayreuth, Chair of Engineering Thermodynamics and Transport Processes (LTTT), Center of Energy Technology (ZET), Universitätsstraße 30, 95447 Bayreuth, Germany

[2]Technical UAS Amberg-Weiden, Center of Excellence for Cogeneration Technologies (CECoGen), Kaiser-Wilhelm-Ring 23, 92224 Amberg, Germany

*tobias.popp@uni-bayreuth.de

ABSTRACT

Organic Rankine Cycle (ORC) systems are a widespread technology for recovering the waste heat of low to medium temperature energy sources. Despite the fact that they are commercially used in a wide range of applications, the data situation concerning the thermodynamic performance of the different components of those plants is rather poor, especially regarding part-load operation. In the scope of the present paper, comprehensive experimental results of an ORC test rig with hexamethyldisiloxane (MM) as working fluid and a Quasi-Impulse Cantilever turbine as expansion machine are presented. For preheating, evaporating and superheating the working fluid, a Plate & Shell heat exchanger was applied. Exhaust gas from a propane gas burner served the test rig as heat source. At design point, MM was evaporated at a pressure level of 6 bar. By expanding the working fluid to 0.32 bar, an electrical power output of approx. 12 kW was generated. All main components of the cycle, i.e. heat exchangers, feed pump and turbine, were analyzed concerning their thermodynamic operational behavior. Part-load operating points down to 50% of the ORC design mass flow rate were considered. Due to the fixed swallowing capacity of the used turbine, a decrease in mass flow rate was always associated with a drop of the evaporation pressure of the cycle. Experimental results for each component of the ORC system were analyzed. The corresponding off-design characteristics were implemented in a commercial cycle modelling tool for quasi-stationary simulations. Hence, a digital twin of the experimental test rig was provided. In this simulation model, it could be shown that WHR efficiency at 50% design mass flow rate could be improved from 4.6% to 7.2% by substituting the fixed geometry turbine by one with adjustable swallowing capacity.

1 INTRODUCTION

ORC systems are well known for their ability to recover the waste heat of low to medium temperature heat sources. Despite the widespread application of ORC solutions for waste heat recovery (WHR) in different fields of industry, the availability of scientific data about the energy balance of the cycle's main components is rather poor, especially when it comes to part-load operation. There are various recent publications focusing on the part-load behavior of experimental ORC units in literature (Bianchi *et al.*, 2019; Carraro *et al*., 2020; Unamba *et al*., 2017). Mainly, these investigations are focused on small ORC units (< 3 kW$_{el}$) with rather low temperatures of the heat source and thereby favoring the application of volumetric expanders. In contrast, the authors of the present paper present the energy balance of a medium-temperature ORC system (approx. 12 kW$_{el}$), using the working fluid hexamethyldisiloxane (MM) and a Quasi-Impulse Cantilever turbine as expansion machine. Operating points down to 50% of the design working fluid mass flow rate (0.32 kg/s) were considered. From the experimentally determined data, off-design characteristics of the feed pump, the evaporator, the turbine and the condenser were derived.

As experimental investigations tend to be rather expensive, simulative investigations of ORCs become more and more important in research. Experimental validation of the developed off-design models by

means of experimental data is a main issue in the context of a reliable prediction of the ORC's performance. Hence, this topic is tackled in different recent publications (Petrollese *et al.*, 2020; Dickes *et al.*, 2017; Mazzi *et al.*, 2015). According to Lecompte *et al.* (2018), the models can be divided into black box, gray box and white box models. While black box models apply a simple data regression and hence relate the model inputs directly to the model outputs, white box models apply the underlying physical laws and are therefore more accurate. The major drawback of white box models is that they are, in contrast to the simple, less accurate black box models, computationally expensive. Gray box models are the compromise in between these two models and apply semi-empirical correlations, which are physically based. In the present paper, the experimentally derived off-design characteristics of the ORC components were used in a simulation of the ORC plant in Aspen Plus v10. In this way, a digital twin of the existing research plant was created. Most of the components were modeled as black boxes. However, for the heat exchanger, which is used as an economizer, evaporator and superheater (in the following, for the sake of simplicity, referred to as "evaporator"), a semi-empirical approach was chosen. This power law approach has already been applied by other authors (Manente *et al.*, 2013; Capra and Martelli, 2015). However, the named publications did not consider the application of a Plate & Shell heat exchanger. The aim was to adapt the semi-empirical approach for the present Plate & Shell heat exchanger application and design by using the experimental data. The digital twin of the plant was used to predict the part-load behavior of the cycle, when the turbine inlet pressure is held constant by an adjustable turbine geometry, which has already been considered by other authors (Manente *et al.*, 2013; Hu *et al.*, 2015; Schuster *et al.*, 2020). The promising result of this simulation is the motivation for current investigations (Streit *et al.*, 2021) and the future development of a turbine with adjustable swallowing capacity.

2 METHODOLOGY

In the following, an overview about the used methodology is given. Firstly, the main components of the ORC are introduced and the applied equations for calculating their efficiency are shown. Afterwards, the constitution of the ASPEN Plus model is presented, together with the implemented constraints and the applied mathematical fit functions of the experimental data.

2.1 Introduction of the plant & energy balance of the ORC's main components

Table 1 lists the main components of the investigated ORC research plant. In order to generate the temperatures and mass flow rates occurring at WHR applications in industry, a propane gas burner in combination with several fans was used. For pumping the low-pressure fluid to the required pressure level, two pumps were applied. The main feed pump, a diaphragm pump, was reused from a former plant. In the current plant, an additional centrifugal pump as booster pump was required to avoid cavitation. For preheating, evaporating and overheating, a Plate & Shell heat exchanger from the manufacturer GESMEX is used. As expansion machine, a Quasi-Impulse Cantilever turbine was used, which has already been presented in previous publications (Weiß *et al.*, 2018; Weiß *et al.*, 2020). The plate heat exchanger serving as condenser was provided by ALPHA LAVAL. An air cooler outside of the building is used to cool the intermediate water/glycol cycle, which serves as heat sink for the condenser.

Table 1: Main components of the investigated ORC test rig

Component	Type
Heat supply	Propane gas burner
Pumps	Centrifugal & piston diaphragm pump in series
"Evaporator"	Plate & Shell type heat exchanger
Expander	Quasi-Impulse Cantilever turbine
Condenser	Plate heat exchanger
Heat sink	Air cooler

Already in previous publications (Weiß *et al.*, 2018; Weiß *et al.*, 2020), data generated with this test rig, with focus on turbine analysis, was published by the authors. To enable a comprehensive energy balance for the system, the research plant was equipped with additional measurement sensors. In the following, the equations used for calculating the efficiencies of the main components are listed. For calculating the thermodynamic properties of the working fluids as well as those of the exhaust gas, the REFPROP Data Base, Version 9.1 (Lemmon *et al.*) was used.

The pump efficiency was calculated as the ratio of hydraulic power added to the working fluid and the electrical power consumption of the two pumps. Thus, "pump efficiency" stands for total efficiency of the two pumps and the two electric drives.

$$\eta_{pump} = \frac{\dot{V}_{MM} \cdot \Delta p_{pump}}{P_{el,pump}} \cdot 100\% \qquad (1)$$

Where $\dot{V}_{MM}$ is the volumetric flow rate of the working fluid MM, Δp_{pump} the pressure difference over the two pumps and $P_{el,pump}$ the electrical power, consumed by the two pump drives.

The evaporator efficiency was defined as the ratio of the enthalpy flux absorbed from the high-pressure working fluid and the enthalpy flux delivered by the exhaust gas. For calculating the enthalpy fluxes of the exhaust gas, the composition (H_2O and CO_2) was measured by means of an FTIR analyzer. The contents of the remaining components were calculated based on CO_2 content and the corresponding chemical reactions. Due to a very high excess air for the present combustion process, the assumption of a complete combustion is legitimate.

$$\eta_{evaporator} = \frac{\dot{H}_{MM,EV,out} - \dot{H}_{MM,EV,in}}{\dot{H}_{EG,in} - \dot{H}_{EG,out}} \cdot 100\% \qquad (2)$$

With $\dot{H}_{MM,EV,in}$ & $\dot{H}_{MM,EV,out}$ being the inlet and outlet enthalpy fluxes of the high-pressure working fluid at the evaporator (EV) and $\dot{H}_{EG,in}$ & $\dot{H}_{EG,out}$ representing the exhaust gas enthalpy fluxes.

For evaluating the turbine, the total-to-static isentropic efficiency was used. To avoid the determination of a too optimistic efficiency due to heat losses, the turbine outlet temperature was not used to calculate the turbine efficiency. Instead, based on a known efficiency characteristic of the electronics (generator & power electronics), the turbine shaft power could be calculated based on the electrical power output. This approach has already been used in previous publications of the authors (Weiß *et al*., 2018; Weiß *et al.*, 2020).

$$\eta_{turbine} = \frac{\frac{P_{el,turbine}}{\eta_{electronics}}}{\dot{m}_{ORC} \cdot \Delta h_{is,turbine}} \cdot 100\% \qquad (3)$$

$P_{el,turbine}$ is the electrical power at the outlet of the feed-in unit, $\eta_{electronics}$ the aforementioned common efficiency of generator and power electronics, $\dot{m}_{ORC}$ the mass flow rate of the working fluid and $\Delta h_{is,turbine}$ the isentropic enthalpy drop over the turbine.

The efficiency of the condenser was calculated as the heat flux added to the cooling water (CW) in relation to the enthalpy flux difference, produced by condensing the low-pressure working fluid in the condenser (CD).

$$\eta_{condenser} = \frac{\dot{m}_{CW} \cdot c_{p,CW} \cdot \Delta T_{CW}}{\dot{H}_{MM,CD,in} - \dot{H}_{MM,CD,out}} \cdot 100\% \qquad (4)$$

With $\dot{m}_{CW}$ as the mass flow rate of cooling water, $c_{p,CW}$ as isobaric heat capacity of the cooling water and ΔT_{CW} as temperature difference of the cooling water over the condenser. $\dot{H}_{MM,CD,in}$ and $\dot{H}_{MM,CD,out}$ represent the inlet and outlet enthalpy fluxes of the low-pressure working fluid at the condenser.

2.2   The derived simulation model

Figure 1 shows the main flow sheet of the simulation model. For the heat exchangers (EVAP and COND), in a first approach, a simple model, only calculating the energy balance without consideration of the geometrical data was used. Pressure losses were not included here. The simulation was based on mathematical data fits (polynomial functions of first to third degree) of the experimental results. For calculating the component properties, the Peng-Robinson equation of state was applied. To model the experimental data fits, different design specifications, only depending on the working fluid mass flow

rate, were integrated into the simulation. The following design specifications were considered in the simulation to approximate the measured plant behavior:

- Exhaust gas (XG-IN) composition (CO_2, H_2O, N_2, O_2), which was determined by FTIR measurements
- Exhaust gas mass flow rate
- Exhaust gas inlet temperature (XG-IN)
- Efficiency of the pumps (simulated as a single pump)
- Evaporator (EVAP) efficiency as heat leakage of the MHeatX block
- Condenser (COND) efficiency as heat leakage of the MHeatX block
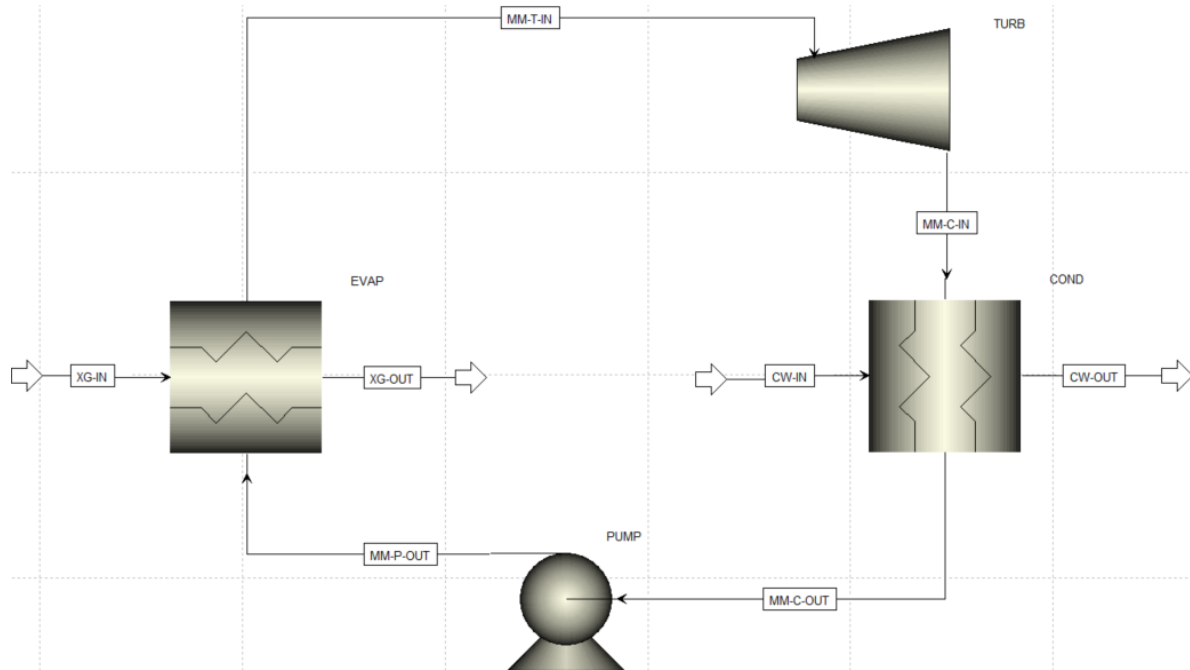- Subcooling of the working fluid (MM-C-OUT) in the condenser

Figure 1: Main Flowsheet of the ASPEN Plus simulation model of the ORC

Apart from the named mathematical fit functions, for the turbine and the evaporator, more detailed off-design constraints were considered:

Theoretically, due to a choking nozzle, the swallowing capacity of the supersonic turbine with constant nozzle area would be constant for the different operating points, as discussed in (Streit *et al.*, 2021):

$$\frac{\dot{m}_{ORC} \cdot \sqrt{T_{total}}}{p_{total} \cdot \sqrt{R_i}} = const. \tag{5}$$

However, from the experimental data, it could be derived that the swallowing capacity (in the definition from above), slightly depends on the mass flow rate (caused by varying superheating (Weiß *et al.*, 2018)). Hence, another design specification for this relation was implemented. The isentropic efficiency of the turbine (see Equation 3) as a function of the pressure ratio was also integrated into the simulation. Another constraint was the definition of the efficiency of the electrical conversion chain in dependency of the power output. The evaporator, firstly simulated as black box, was in a later step described by a (semi-empirical) power law (in a HeatX model). Hence, for the evaporator, a gray box model was introduced. The transferred heat in the evaporator could be calculated as

$$\dot{Q}_{evaporator} = U \cdot A \cdot LMTD \tag{6}$$

with U as heat transfer coefficient, A as heat transfer area and $LMTD$ as logarithmic mean temperature difference (counterflow). As already applied by other authors (Manente *et al.*, 2013; Capra and Martelli, 2015), the overall heat transfer coefficient in U an operating point deviating from the design point (DP) could be calculated as:

$$U = U_{DP} \cdot \left(\frac{\dot{m}}{\dot{m}_{DP}}\right)^n \tag{7}$$

With the exponent n, which is specific to the investigated heat transfer problem and U_{DP} as overall heat transfer coefficient in design point. In the present publication, this approach was marginally modified by using $U \cdot A$, instead of just U in the power law:

$$U \cdot A = U_{DP} \cdot A \cdot \left(\frac{\dot{m}}{\dot{m}_{DP}}\right)^n \tag{8}$$

From the experimental results, $U \cdot A$ values can be derived. By means of the simulation, the best-fitting n for the considered heat transfer problem was determined.

As a first application of the simulation model, the waste heat recovery efficiency for constant and varying turbine inlet pressure was analyzed. This efficiency is given as:

$$\eta_{WHR} = \frac{P_{el,turbine}}{\dot{H}_{EG,in} - \dot{H}_{EG,out}} \cdot 100\% \tag{9}$$

3   RESULTS

3.1   Off-design characteristics of the main components

In previous publications, the authors have already shown extensive experimental results concerning the off-design efficiency of the Quasi-Impulse Cantilever turbine (Weiß *et al.*, 2018; Weiß *et al.*, 2020). However, the remaining components of the cycle have not been analyzed in detail yet. In the present paper, besides more detailed turbine investigations, characteristic curves of the heat exchangers and the pump are provided, additionally. In Figure 2, the efficiency characteristics of all main components of the ORC for a mass flow rate down to 50% of the design (0.32 kg/s) are shown. The data points derive from a measurement campaign with 7 measurement days in total. As already described, the condensing pressure was, besides the dependency of the ambient temperature, varied intentionally by different working fluid filling quantities in the plant. In Figure 2(a), the course of the pump efficiency in dependency of the mass flow rate is shown. The fact that the reused main pump from a former project does not perfectly match the pumping task explains the rather low total pump efficiency of approx. 30% at design point. In general, the measurement data shows a good reproducibility and the course matches the expectations. In Figure 2(b), the evaporator efficiency is shown as a function of the ORC mass flow rate. Interestingly, the Plate & Shell heat exchanger shows a weak dependency on the cold sides' mass flow rate. The highest efficiency of approx. 83% was reached at design mass flow rate. The condenser efficiency in dependency of the working fluid mass flow rate is depicted in Figure 2(c). To create this graph, firstly, a fit for the heat flux added to the cooling water was derived from the measurement data. Secondly, the fit for the cooling water heat flux was divided by a fit for the condensing of the low-pressure fluid. This enabled the derivation of quite a clear trend, despite the rather low temperature differences in the cooling water, which resulted in a strong scattering of the heat added to the cooling water. Looking at the graph, a minimal condenser efficiency of approx. 92.5% can be observed at 105% mass flow rate. In Figure 2(d) the total-to-static isentropic turbine efficiency is analyzed. In contrast to the other 3 graphs, it shows the turbine efficiency as function of the pressure ratio, not the mass flow rate. From the performed experiments, it could clearly be deduced that the isentropic turbine efficiency does not depend on the working fluid mass flow rate. Even when targeting the same pressure ratio with different inlet pressures i.e. mass flow rates, the resulting turbine efficiency is almost identical (Figure 3). This turbine efficiency graph (Fig. 2d) is, from the authors' point of view, unique and may be a valuable contribution for the simulation community.
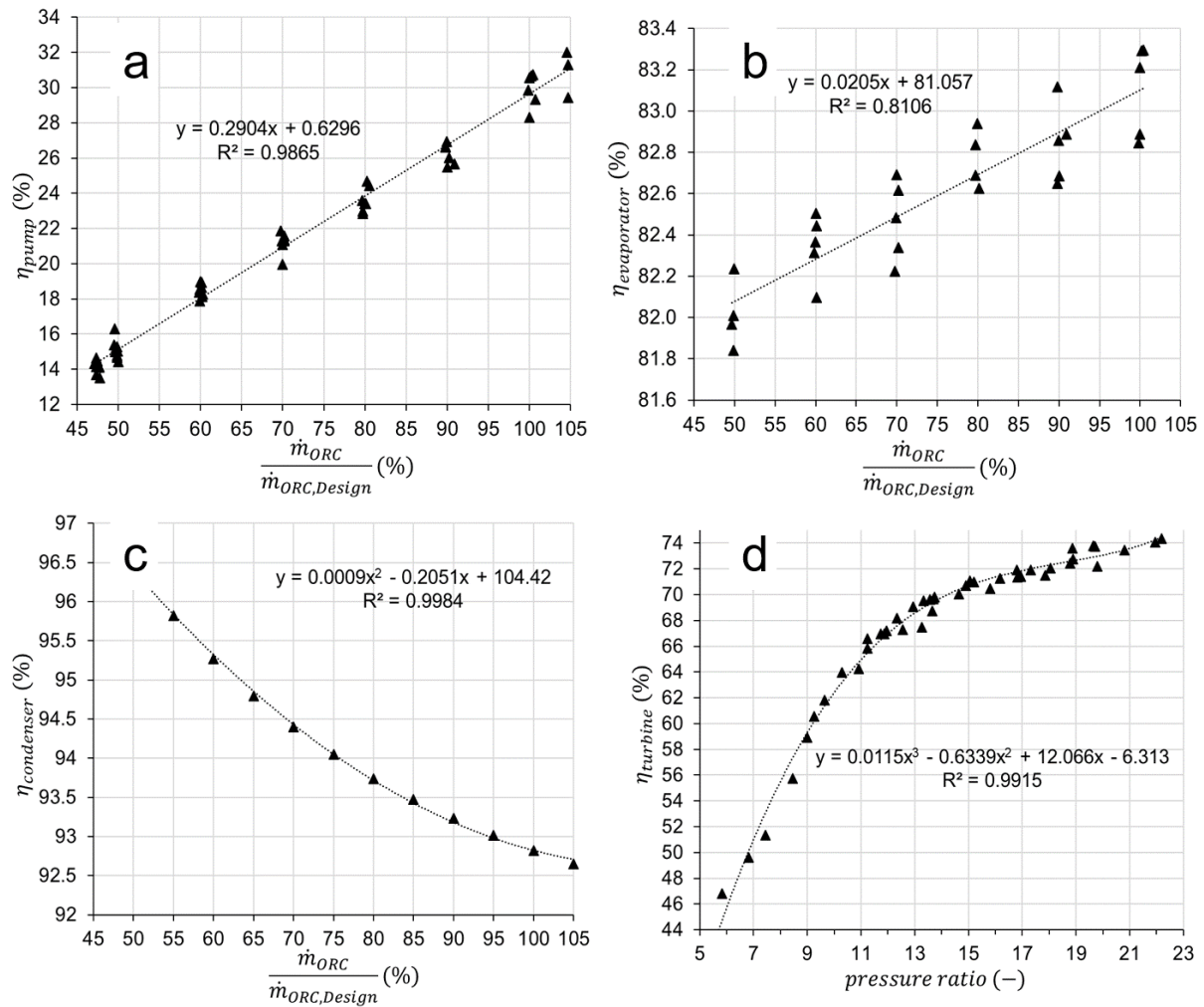
Figure 2: Pump (a), evaporator (b) and condenser (c) efficiency as function of reduced working fluid mass flow rate, isentropic efficiency (d) as function of pressure ratio

The radial inflow Cantilever turbine is introduced and discussed in detail in (Weiß *et al.*, 2018). The shape of its efficiency characteristic is mainly determined by the operational behaviour of its supersonic Laval nozzles. These nozzles work at a pressure ratio (*PR*) of 13 and the overall turbine design pressure ratio is 18.3. Thus, a portion of the pressure or enthalpy drop, respectively is processed by the centrifugal pressure field in the radial cantilever wheel. In a certain range of the overall turbine *PR* ($13 < PR < 22$), the change of this pressure ratio can be compensated by adjusting the turbine rotational speed and thereby varying the intermediate pressure between nozzle exit and wheel inlet. The design *PR* of the nozzles can be almost maintained. For overall turbine *PR* < 13, the nozzle *PR* must drop significantly below 13 and compression shocks combined with flow separations are most likely to appear in the divergent part of the nozzles. Nevertheless, for a small highly-loaded turbine with a power output of about 12 kW$_{el}$, the measured peak efficiency of approx. 74% is a very satisfactory performance.
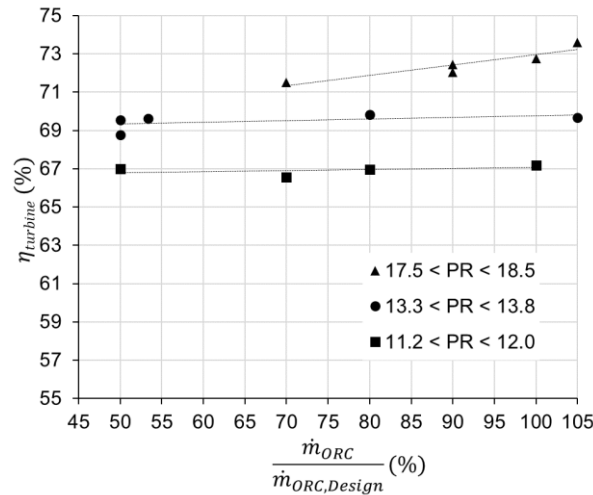
Figure 3: Total-to-static turbine efficiency as a function of reduced mass flow rate for different almost constant pressure ratios (*PR*)

3.2   Semi-empirical model for the evaporator

As already described, one aim of the present publication was to approximate the actual $U \cdot A$ values for the evaporator from the experiments by a semi-empirical model, instead of just a black box model. In the following figure, different values for the exponent in equation 8 were used in the simulation and the agreement of the corresponding $U \cdot A$ values with experimental results was analyzed. The exponents 0.15 and 0.66 were chosen as reference, according to Tofollo *et al*. (2012) valid for a subcritical preheater & evaporator and a supercritical evaporator. As it becomes obvious, the exponent $n = 0.4$ shows the best agreement with the experimental values for the Plate & Shell heat exchanger.
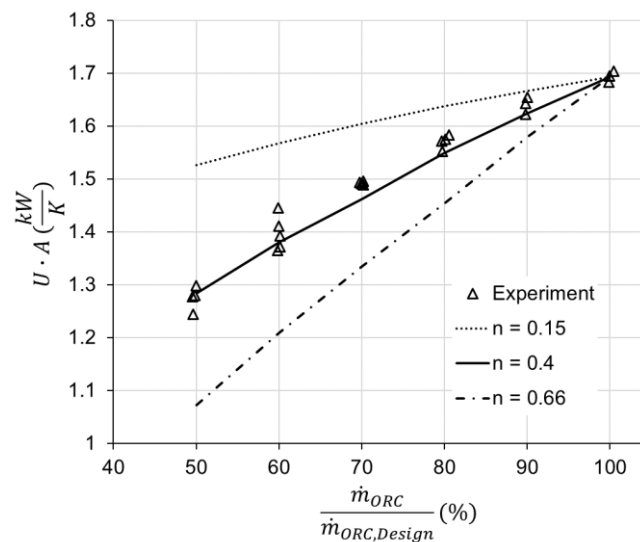

Figure 4: *U·A* values for the evaporator for application of the power law

3.3   Prediction of the off-design performance with constant turbine inlet pressure

From Equation 5 it becomes obvious that the off-design operation of an ORC unit with a turbine as expansion machine is always associated with a decrease in turbine inlet pressure (constant swallowing capacity, CSC), which has a negative influence on the waste heat recovery efficiency. In the following (Figure 5), power (a) as well as waste heat recovery efficiency (b) from the experiments are compared to the simulated results. In addition, a simulation is performed, where the turbine inlet pressure is held constant (CTIP). In practice, this behavior could be achieved by a turbine with adjustable swallowing

capacity (see (Streit *et al.*, 2021)). The simulation for constant swallowing capacity shows a good agreement with the experimental results in terms of turbine power output and waste heat recovery efficiency. The main reason for the deviation is that during the considered measurement, the outlet pressure slightly varies between 0.23 and 0.31 bar, whereas it is assumed as constantly at 0.32 bar (design outlet pressure) in the simulation. Generally, the course of the measurements is satisfactorily approximated by the simulations. This encourages the authors to apply it for performance predictions of not measured operational points like those with constant turbine inlet pressure. From the graph for constant turbine inlet pressure (CTIP), a significant improvement of the waste heat recovery efficiency in part-load can be expected. According to the simulation, the waste heat recovery efficiency is in part-load even higher than for the design operating point. The reason for this behavior is an increase of the simulated evaporator efficiency for the part-load operating points, due to the changed pressure level. In context of the results for constant turbine inlet pressure, a turbine with variable geometry (Streit *et al.*, 2021) and thereby adjustable swallowing capacity is currently under development. A comparison of experimentally achieved waste heat recovery efficiencies in part-load, when applying this turbine with variable swallowing capacity, is planned for future investigations.
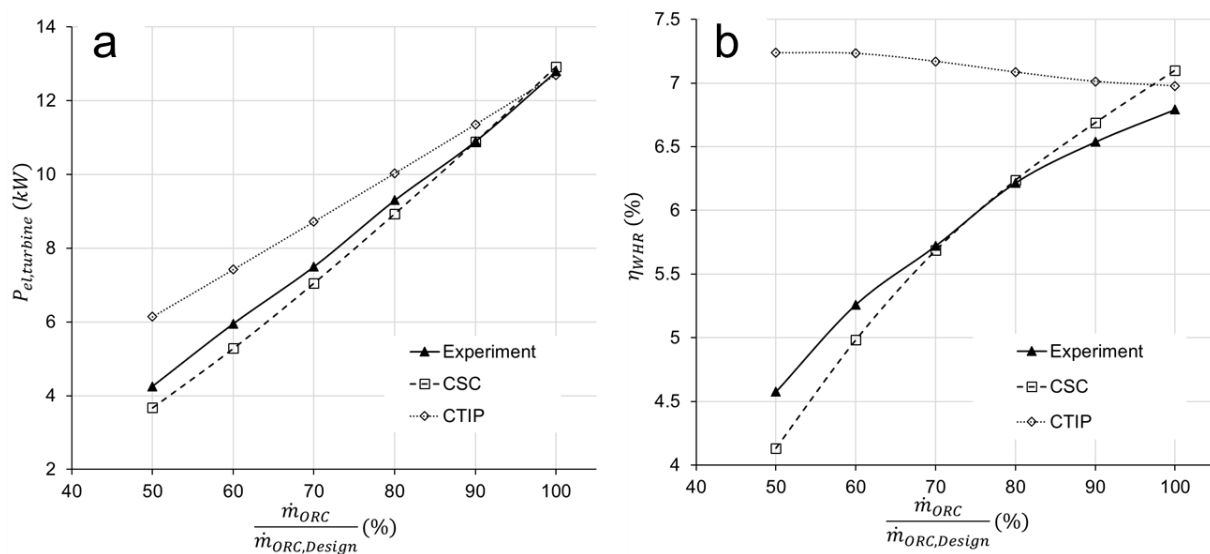

Figure 5: Electrical power output of the turbine and waste heat recovery efficiency for constant swallowing capacity (CSC) and constant turbine inlet pressure (CTIP).

4   CONCLUSIONS

Detailed off-design characteristics of the feed pump, the heat exchangers and the turbine of a medium-temperature ORC test rig were presented. The resulting data fits of the experimental results were used in a simple ASPEN Plus simulation to create an experimentally validated model or digital twin for off-design investigations. The simulation, which is mainly based on black box models of the main components, was improved by the introduction of a semi-empirical approach for the evaporator. By using the detailed experimental results, the authors were able to adapt the power law approach for the evaporator for the present heat transfer problem. The developed simulation model for the ORC was applied to show the effect of a constant turbine inlet pressure on the waste heat recovery efficiency under off-design conditions. The WHR efficiency at 50% design mass flow rate could be improved from 4.6% to 7.2% by substituting the fixed geometry turbine by one with adjustable swallowing capacity. The promising results encourage the authors to continue with their development of a supersonic turbine with adjustable swallowing capacity for the application in waste heat recovery (Streit *et al.*, 2021).

NOMENCLATURE

A	heat transfer area	(m²)
c_p	isobaric heat capacity	(J/kg/K)
h	specific enthalpy	(J/kg)
$\dot{H}$	enthalpy flux	(J/s)
$LMTD$	logarithmic mean temperature difference	(K)
$\dot{m}$	mass flow rate	(kg/s)
η	efficiency	(-)
p	pressure	(Pa)
P	power	(W)
PR	pressure ratio	(-)
T	temperature	(K)
U	overall heat transfer coefficient	(W/m²/K)
$\dot{V}$	volume flow rate	(m³/s)

Subscript

CD	condenser	el	electrical
CW	cooling water	EV	evaporator
DP	design point	is	isentropic
EG	exhaust gas	WHR	waste heat recovery

REFERENCES

Bianchi, M., Branchini, L., Casari, N., Pascale, A. de, Melino, F., Ottaviano, S. et al, 2019, Experimental analysis of a micro-ORC driven by piston expander for low-grade heat recovery, In: *Applied Thermal Engineering* 148, p. 1278–1291, DOI: 10.1016/j.applthermaleng.2018.12.019.

Capra, F., Martelli, E., 2015, Numerical optimization of combined heat and power Organic Rankine Cycles – Part B: Simultaneous design & part-load optimization, In: *Energy* 90, p. 329–343.

Carraro, G., Bori, V., Lazzaretto, A., Toniato, G., Danieli, P., 2020, Experimental investigation of an innovative biomass-fired micro-ORC system for cogeneration applications, In: *Renewable Energy* 161, p. 1226–1243, DOI: 10.1016/j.renene.2020.07.012.

Dickes, R., Dumont, O., Daccord, R., Quoilin, S.; Lemort, V., 2017, Modelling of organic Rankine cycle power systems in off-design conditions: An experimentally-validated comparative study, In: *Energy* 123, p. 710–727, DOI: 10.1016/j.energy.2017.01.130.

Hu, D., Zheng, Y., Wu, Y., Li, S., Dai, Y., 2015, Off-design performance comparison of an organic Rankine cycle under different control strategies, In: *Applied Energy* 156, p. 268–279.

Lecompte, S., Gusev, S., Vanslambrouck, B., Paepe, M. de, 2018, Experimental results of a small-scale organic Rankine cycle: Steady state identification and application to off-design model validation. In: *Applied Energy* 226, p. 82–106, DOI: 10.1016/j.apenergy.2018.05.103.

Lemmon, E.W., Huber, M.L., McLinden, Mark O., NIST Standard Reference Database 23: Reference Fluid Thermodynamic and Transport Properties-REFPROP, Version 9.1. available online: https://www.nist.gov/publications/nist-standard-reference-database-23-reference-fluid-thermodynamic-and-transport.

Manente, G., Toffolo, A., Lazzaretto, A., Paci, M., 2013, An Organic Rankine Cycle off-design model for the search of the optimal control strategy, In: *Energy* 58, p. 97–106, DOI: 10.1016/j.energy.2012.12.035.

Mazzi, N., Rech, S., Lazzaretto, A., 2015, Off-design dynamic model of a real Organic Rankine Cycle system fuelled by exhaust gases from industrial processes. In: *Energy* 90, p. 537–551.

Petrollese, M., Dickes, R., Lemort, V.,2020, Experimentally-validated models for the off-design simulation of a medium-size solar organic Rankine cycle unit, In: *Energy Conversion and Management* 224, p. 113307, DOI: 10.1016/j.enconman.2020.113307.

Schuster, S., Markides, C.N., White, A.J., 2020, Design and off-design optimisation of an organic Rankine cycle (ORC) system with an integrated radial turbine model, In: *Applied Thermal Engineering* 174, p. 115192, DOI: 10.1016/j.applthermaleng.2020.115192.

Streit, P., Popp, T., Winkler, J., Scharf, R., Weiβ, A.P., 2021, Numerical and Experimental Investigation of Different Technologies for Adjusting the Swallowing Capacity of a Cantilever ORC Turbine, In: 19th Conference on Power System Engineering, PSE 2020, Pilsen, Czech Republic, 8–10 September 2020: AIP Publishing (AIP Conference Proceedings).

Toffolo, A., Lazzaretto, A., Manente, G., Paci, M., 2012, An Organic Rankine Cycle off-design model for the search of the optimal control strategy. In: Proceedings of ECOS 2012 - The 25th International Conference on Efficiency, Cost, Optimization and Simulation of Energy Conversion Systems and Processes, Firenze University Press, 2012.

Unamba, C.K.; White, M.; Sapin, P., Freeman, J., Lecompte, S., Oyewunmi, O.A., Markides, C.N., 2017, Experimental Investigation of the Operating Point of a 1-kW ORC System, In: *Energy Procedia* 129, p. 875–882, DOI: 10.1016/j.egypro.2017.09.211.

Weiß, A.P., Novotný, V., Popp, T., Streit, P., Špale, J., Zinn, G., Kolovratník, M., 2020, Customized ORC micro turbo-expanders - From 1D design to modular construction kit and prospects of additive manufacturing, In: *Energy* 209, p. 118407, DOI: 10.1016/j.energy.2020.118407.

Weiß, A.P., Popp, T., Müller, J., Hauer, J., Brüggemann, D., Preißinger, M., 2018, Experimental characterization and comparison of an axial and a cantilever micro-turbine for small-scale Organic Rankine Cycle, In: *Applied Thermal Engineering* 140, p. 235–244. DOI: 10.1016/j.applthermaleng.2018.05.033.

ACKNOWLEDGEMENT